Solution Structures of Copper Coordination Compounds Containing Ligands with Ether or Thioether Donors

Huikang Wu and C. Robert Lucas*

Department of Chemistry, Memorial University of Newfoundland, St. John's, Newfoundland, Canada A1B 3X7

Received May 15, 1992

The ligand 1,9-bis(2-thienyl)-5-oxa-2,8-dithianonane (L3) and the complexes $CuCl_2$·2L1, $(CuCl_2$·L2$)_2$, and $CuCl_2$·L3 (L1 = 1,6-bis(2-thienyl)-2,5-dithiahexane; L2 = 1,9-bis(2-thienyl)-2,5,8-trithianonane) have been prepared. The solid-state molecular structures of $CuCl_2$·2L1 and $CuCl_2$·L3 have been obtained by X-ray methods. For monoclinic $CuCl_2$·2L1: space group $P2_1/c$; a = 14.899(3), b = 7.7881(6), c = 13.586(2) Å; β = 102.29(1)°; Z = 4; R = 0.043, R_w = 0.042 for 1943 reflections. The copper is in a centrosymmetric, tetragonally elongated six-coordinate environment. For orthorhombic $CuCl_2$·L3: space group *Pnma*; a = 12.562(4), b = 17.435(2), c = 8.767(2) Å; Z = 4; R = 0.050, R_w = 0.043 for 785 reflections. The copper is in a distorted trigonal bipyramidal environment and lies in a plane of symmetry also containing the oxygen and the two chlorine atoms. All three complexes have been examined in the solid state and in dichloromethane, acetonitrile, and *N*,*N*-dimethylformamide solutions by a combination of solution conductance studies, cyclic voltammetry, electronic, IR, and ESR spectroscopy, and magnetic susceptibility measurements. Conclusions are reached concerning changes in the structure of copper's coordination sphere that occur as a result of dissolving. The extent and nature of these changes depend both upon the identity of the solvent and upon the concentration of the solutions.

Introduction

For several years we have been interested in structural effects in coordination and organometallic complexes of sulfur-containing ligands,[1-3] and recently we described 1,4-heteroatom binding site fluxionality[3,4] as well as the effects of anion coordination, solvation, and removal or alteration of apical donor atoms in square pyramidal complexes of copper.[5] As a result of these interests, we have frequently encountered the problem of having to extrapolate from the known solid-state structure of a compound to its probable solution structure. We are not alone in facing this problem. For example, attempts to develop simple models of the active sites in metalloenzymes are based on an assumption in most cases that a structure in the solid state as revealed by X-ray crystallography bears a strong resemblance to that in solution, at least within the coordination sphere of the metal. Particularly in the case of "type 1" copper centers in "blue" copper proteins, considerable success has accompanied such attempts although it has not yet been possible to duplicate simultaneously all of the enzymes' properties. There are several reasons for this, and at least some are related to uncertainties about the solution structures of the model compounds. In an attempt to resolve this problem, studies of complexes with biologically relevant ligands in both aqueous and nonaqueous media have been undertaken by several groups.[6-8] Since thioether sulfur is coordinated to copper at the active sites in enzymes such as plastocyanin[9] and azurin,[10] we have examined some thioether complexes of copper(II) in the solid state and in the nonaqueous solvents CH_2Cl_2, CH_3CN, and $HCON(CH_3)_2$ in order to evaluate any changes that occur in their structures upon dissolving. The ligands, their designations, and the position identifiers used for the remainder of this report are shown in Figure 1.

Experimental Section

Commercially available reagents were obtained from the Aldrich Chemical Co. Inc. or from Morton Thiokol Alfa Products Inc. and were used without further purification. Those used for conductivity or cyclic voltammetry measurements were spectroscopic grade. We have previously reported preparations for ligands L1 and L2.[4] Spectroscopic data were obtained by using the following instruments: IR, Perkin-Elmer Model 283 or Mattson Polaris FT; UV/vis, Cary Model 17; ESR, Bruker ESP-300 X-band spectrometer operating at ~9.5 GHz. Solution "glasses" for ESR measurements were prepared by plunging sealed capillaries containing ~10^{-4} mol/L solutions in liquid nitrogen. Magnetic susceptibility data were obtained at room temperature by the Faraday method. Electrochemical measurements were carried out under a nitrogen atmosphere at room temperature using a BAS CV27 Voltammograph and a Houston 2000 Omnigraph X-Y recorder. Solution concentrations were 10^{-3} mol/L in complex and 0.1 mol/L in supporting electrolyte (tetraethylammonium perchlorate). Voltammograms were recorded using a glassy carbon working electrode that was prepolished with 0.3-μm Al_2O_3, a platinum counter electrode, and an aqueous saturated calomel reference electrode checked periodically relative to a 1.0 × 10^{-3} mol/L solution of ferrocene in dimethyl sulfoxide containing 0.1 mol/L tetraethylammonium perchlorate for which the ferrocene/ferrocenium reduction potential was 400 mV. The reference electrode was separated from the bulk of the solution by a porous Vycor tube. Junction potential corrections were not used. Conductance data were obtained by using a General Radio Co. Type 1605-AH bridge with impedance comparator and a constant-temperature bath adjusted to 25 °C. X-ray diffraction data were collected by using a Rigaku AFC6S diffractometer. Analyses were performed by Canadian Microanalytical Service Ltd.

Preparative Details. $C_{14}H_{18}OS_4$, Ligand L3. Sodium (4.60 g, 0.200 mol) was dissolved in commercial absolute ethanol (300 mL) under an atmosphere of dry nitrogen, and bis(2-mercaptoethyl) ether (10.4 g, 0.0750 mol) was added slowly. The resulting mixture was heated to reflux, and a solution of 2-(chloromethyl)thiophene[11] (19.9 g, 0.150 mol) in ethanol

* Corresponding author. Phone: (709) 737-8118.

(1) Lucas, C. R.; Liu, S.; Thompson, L. K. *Inorg. Chem.* **1990**, *29*, 85.
(2) Lucas, C. R.; Liu, S.; Newlands, M. J.; Charland, J. P.; Gabe, E. J. *Can. J. Chem.* **1990**, *68*, 644.
(3) Liu, S.; Lucas, C. R.; Newlands, M. J.; Charland, J. P. *Inorg. Chem.* **1990**, *29*, 4380.
(4) Wu, H.; Lucas, C. R. *Inorg. Chem.* **1992**, *31*, 2354.
(5) Liu, S.; Lucas, C. R.; Hynes, R. C.; Charland, J. P. *Can. J. Chem.* **1992**, *70*, 1773.
(6) Zoeteman, M.; Bouwman, E.; deGraaff, R. A. G.; Driessen, W. L.; Reedijk, J.; Zanello, P. *Inorg. Chem.* **1990**, *29*, 3487. E
(7) Rorabacher, D. B.; Bernardo, M. M.; Vande Linde, A. M. Q.; Leggett, G. H.; Westerby, B. C.; Martin, M. J.; Ochrymowycz, L. A. *Pure Appl. Chem.* **1988**, *60*, 501.
(8) Addison, A. W. *Inorg. Chim. Acta* **1989**, *162*, 217.
(9) Guss, J. M.; Freeman, H. C. *J. Mol. Biol.* **1983**, *169*, 521.
(10) Norris, G. E.; Anderson, B. F.; Baker, E. N. *J. Am. Chem. Soc.* **1986**, *108*, 2784.

0020-1669/93/1332-0526$04.00/0

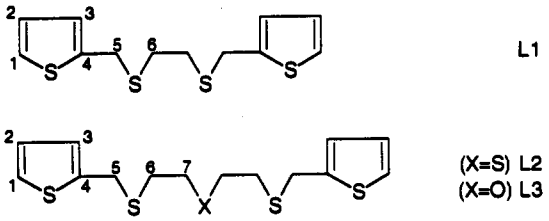

Figure 1. Ligands and position identification scheme.

(50 mL) was added dropwise with stirring. Refluxing was continued for 1 h, during which time a white precipitate appeared. Water (100 mL) was added, the mixture was extracted with chloroform (3 × 200 mL), and the extracts were dried over calcium chloride. Volatiles were removed in vacuo, and the resulting oil was dissolved in a minimum amount of dichloromethane. The solution was filtered, and methanol was added until cloudiness appeared. When the mixture was cooled to −5 °C, formation of a colorless oil occurred: yield 19.3 g (78%). NMR ($CDCl_3$, in ppm from TMS internal standard, position identification from Figure 1): ^1H 7.18 (m, 2H, H1), 6.90 (m, 4H, H2–H3), 3.96 (s, 4H, H5), 3.55 (t, 4H, J = 6.56 Hz, H7), 2.65 (t, 4H, J = 6.56 Hz, H6); ^{13}C 141.8 (C4), 126.5 (C3), 126.1 (C2), 124.8 (C1), 70.3 (C7), 30.8 (C5), 30.7 (C6). Anal. Calcd for $C_{14}H_{18}OS_4$: C, 50.87; H, 5.49. Found: C, 50.70; H, 5.50.

$CuCl_2$·2L1. A solution of L1 (0.573 g, 2.00 mmol) in dichloromethane (5 mL) was added to a solution of $CuCl_2·2H_2O$ (0.171 g, 1.00 mmol) in methanol (25 mL) that had been heated nearly to boiling. Brown crystals formed immediately, and after 10 min of standing they were collected by filtration and washed with methanol (2 mL) and dichloromethane (2 mL). Crystals suitable for X-ray diffraction were obtained by diffusion of ether into a dichloromethane solution of the compound: yield 0.637 g (90%); mp 91 °C dec. Anal. Calcd for $C_{24}H_{28}Cl_2CuS_8$: C, 40.75; H, 3.99; Cl, 10.02. Found: C, 40.69; H, 4.10; Cl, 10.41.

$[CuCl_2·L2]_2$. Solutions of L2 (0.346 g, 1.00 mmol) in dichloromethane (5 mL) and of $CuCl_2·2H_2O$ (0.171 g, 1.00 mmol) in acetonitrile (60 mL) were mixed, and the deep green solution was filtered. The solvent was allowed to evaporate at room temperature until brown crystals were deposited, which were collected by filtration, washed with acetonitrile (2 mL) and then dichloromethane (1 mL), and recrystallized by dissolving in a minimum amount of dichloromethane and then adding diethyl ether slowly until crystallization was initiated: yield 0.361 g (75%); mp 112 °C dec. Anal. Calcd for $C_{28}H_{36}Cl_4Cu_2S_{10}$: C, 34.95; H, 3.77; Cl, 14.74. Found: C, 34.17; H, 3.62; Cl, 16.03.

$CuCl_2$·L3. Solutions of L3 (0.330 g, 1.00 mmol) in dichloromethane (5 mL) and of $CuCl_2·2H_2O$ (0.171 g, 1.00 mmol) in methanol (125 mL) were mixed. Slow evaporation of the resulting solution caused deposition of orange-red crystals suitable for X-ray crystallography: yield 0.349 g (75%); mp 115 °C dec. Anal. Calcd for $C_{14}H_{18}Cl_2CuOS_4$: C, 36.16; H, 3.90; Cl, 15.25. Found: C, 36.30; H, 3.91; Cl, 16.52.

X-ray Studies. A summary of crystal data for $CuCl_2$·2L1 and $CuCl_2$·L3 is given in Table I. Data were collected at 299 K by the ω–2θ scan technique to a maximum 2θ value of 50.0°. Three standards measured after every 150 reflections showed no indication of significant crystal decay. Space groups were determined on the basis of systematic absences, packing considerations, a statistical analysis of intensity distribution, and the successful solution and refinement of the structures. Unit cell parameters (Table I) were determined by a least-squares refinement of the setting angles of 25 reflections (43.11° < 2θ < 44.80° for $CuCl_2$·2L1) or 21 reflections (27.33° < 2θ < 38.10° for $CuCl_2$·L3). Lorentz and polarization factors were applied and corrections were made for absorption. The structure was solved by direct methods[12] and refined by full-matrix least-squares techniques[13] with counting statistic weights. Non-hydrogen atoms were refined anisotropically, while H atom positions were calculated but their parameters were not refined. The final cycle of refinement was based on 1943 ($CuCl_2$·L1) or 785 ($CuCl_2$·L3) observed reflections ($I > 3.00\sigma(I)$) and 200 ($CuCl_2$·2L1) or 106 ($CuCl_2$·L3) variables and converged

Table I. Crystallographic Data for $CuCl_2$·2L1 and $CuCl_2$·L3

	$CuCl_2$·2L1	$CuCl_2$·L3
chem formula	$C_{24}H_{28}Cl_2CuS_8$	$C_{14}H_{18}Cl_2CuOS_4$
fw	707.45	464.99
space group	$P2_1/c$	*Pnma*
T, °C	26	26
a, Å	14.899(3)	12.562(4)
b, Å	7.7881(6)	17.435(2)
c, Å	13.586(2)	8.767(2)
β, deg	102.29(1)	
ρ_{calcd}, g cm^{-3}	1.525	1.608 g cm^{-3}
V, Å^3	1540.4(7)	1920.2(8)
Z	2	4
λ, Å	0.710 69	0.710 69
μ, cm^{-1}	14.22	18.37
R,[a] %	4.3	5.0
R_w,[b] %	4.2	4.3

[a] $R = \Sigma||F_o| - |F_c||/\Sigma|F_o|$. [b] $R_w = [(\Sigma w(|F_o| - |F_c|)^2/\Sigma wF_o^2)]^{1/2}$.

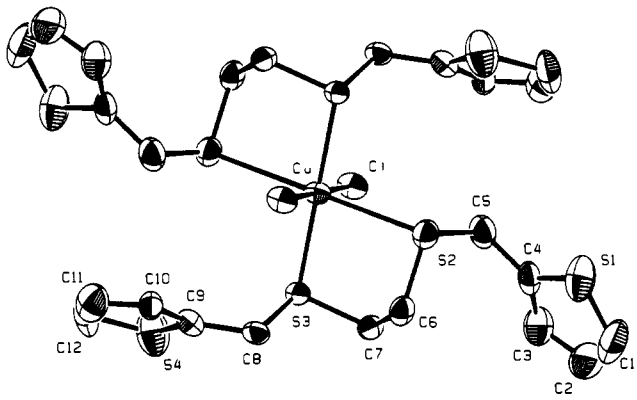

Figure 2. Molecular structure of $CuCl_2$·2L1.

in both cases. All calculations were performed using the TEXSAN[14] crystallographic software of the Molecular Structure Corp., and scattering factors were from the usual source.[15]

Results

The new compounds, ligand L3, and the complexes $CuCl_2$·2L1, $(CuCl_2·L2)_2$, and $CuCl_2$·L3 have been prepared. Structural studies of $CuCl_2$·2L1 and $CuCl_2$·L3 have been conducted by X-ray methods. Results are presented in Figures 2 and 3 and in Tables I–V. The IR, ESR, and electronic spectra and magnetic susceptibilities have been obtained for solid samples of the complexes. In addition, ESR and electronic spectra, cyclic voltammograms, and conductances have been obtained for solutions of the complexes in various solvents. These results are given in Table VI and Figures 4–9 or in the text and will be introduced at appropriate points in the discussion that follows.

Discussion

Solid-state structures of $CuCl_2$·2L1 (Figure 2) and $CuCl_2$·L3 (Figure 3) were determined by X-ray methods. That of $(CuCl_2·L2)_2$ has been inferred from spectroscopic and other data to be discussed shortly due to the fact that crystals suitable for X-ray crystallography could not be grown for this compound.

Molecules of $CuCl_2$·2L1 (Figure 2) are centrally symmetric and have a tetragonally elongated pseudooctahedral coordination sphere about copper that has two long trans Cu–S (2.817(2) Å) bonds and two normal trans Cu–S (2.368(1) Å) bonds as well as two Cu–Cl bonds that are of normal length (2.272(1) Å). These bonds may be compared to those in binuclear $(CuCl_2·BBTE)_2$

(11) Blicke, F. F.; Burckhalter, J. H. *J. Am. Chem. Soc.* **1942**, *64*, 477.
(12) (a) Gilmore, C. J. *J. Appl. Crystallogr.* **1984**, *17*, 42. (b) Beurskens, P. T. Technical Report 1984/1; Crystallography Laboratory: Toernooiveld, 6525 Ed, Nijmegen, The Netherlands, 1984.
(13) Function minimized: $\Sigma w(|F_o| - |F_c|)^2$ where $w = 4F_o^2/\sigma^2(F_o^2)$, $\sigma^2(F_o^2) = [S^2(C + R^2B) + (pF_o^2)^2]/Lp^2$, S = scan rate, C = total integrated peak count, R = ratio of scan time to background counting time, B = total background count, and Lp = Lorentz–polarization factor.
(14) *TEXSAN-TEXRAY Structure Analysis Package*; Molecular Structure Corp.: Woodlands, TX, 1985.
(15) *International Tables for X-ray Crystallography*; Kynoch Press: Birmingham, England, 1974; Vol. IV, Table 2.2A.

Table II. Positional and Thermal Parameters and Equivalent Isotropic Temperature Factors for $CuCl_2$·2L1

atom	x	y	z	B_{eq}[a]
Cu	1/2	1/2	1.0000	2.47(4)
Cl(1)	0.4417(1)	0.2767(2)	0.8988(1)	3.07(6)
S(1)	0.0949(1)	0.7752(3)	0.8629(2)	6.2(1)
S(2)	0.3338(1)	0.6849(2)	0.9638(1)	3.43(7)
S(3)	0.5259(1)	0.6285(2)	0.8505(1)	2.41(5)
S(4)	0.7472(1)	0.6621(3)	0.8279(2)	6.2(1)
C(1)	0.0412(5)	0.835(1)	0.7448(7)	6.7(5)
C(2)	0.0795(6)	0.761(1)	0.6767(6)	6.7(5)
C(3)	0.1534(5)	0.653(1)	0.7164(6)	4.8(4)
C(4)	0.1709(4)	0.6465(8)	0.8191(5)	3.5(3)
C(5)	0.2438(5)	0.5505(9)	0.8881(6)	4.3(3)
C(6)	0.3677(4)	0.8157(7)	0.8685(5)	3.2(3)
C(7)	0.4131(4)	0.7154(8)	0.7956(4)	3.1(3)
C(8)	0.5916(4)	0.8268(7)	0.8727(4)	2.9(2)
C(9)	0.6932(4)	0.7937(7)	0.8999(4)	3.1(3)
C(10)	0.7565(4)	0.8634(8)	0.9820(5)	3.1(3)
C(11)	0.8453(5)	0.804(1)	0.9786(6)	5.3(4)
C(12)	0.8519(4)	0.697(1)	0.9045(6)	5.8(4)

[a] B_{eq} (Å^2) is the mean of the principal axes of the thermal ellipsoid.

Table III. Selected Bond Lengths and Angles in $CuCl_2$·2L1

Distances (Å)			
Cu–Cl(1)	2.272(1)	S(3)–C(7)	1.819(6)
Cu–S(3)	2.368(1)	S(3)–C(8)	1.819(6)
Cu–S(2)	2.817(2)	S(2)–C(6)	1.802(6)
		S(2)–C(5)	1.835(7)
Angles (deg)			
Cl(1)–Cu–Cl(1′)	180.00	S(3)–Cu–S(3′)	180.00
Cl(1)–Cu–S(3)	85.13(5)	S(3)–Cu–S(2)	86.10(5)
Cl(1)–Cu–S(3′)	94.87(5)	S(2)–Cu–S(2′)	180.00
Cl(1)–Cu–S(2)	94.43(5)	S(2)–Cu–S(3′)	93.90(5)
Cl(1)–Cu–S(2′)	85.57(5)		

(BBTE = $BuSCH_2CH_2SBu$),[16] which are 2.308(2), 2.369(2) (Cu–S), and 2.242(2) Å (Cu–$Cl_{terminal}$), those in centrosymmetric, six-coordinate $[Cu(DTH)_2(BF_4)_2]$ (DTH = 2,5-dithiahexane),[17] which are 2.315(2) and 2.319 Å, or those in mononuclear six-coordinate $CuCl_2$·2(1,5,9-trithiacyclododecane), which are 2.447(1), 3.050(1) (Cu–S), and 2.205(4) Å (Cu–$Cl_{terminal}$).[18] As we have previously shown,[19] the expected length of a terminal Cu–S bond on the tetragonal distortion axis of a six-coordinate $CuCl_2$ complex should be ~2.98 Å, so the observed length of 2.817(2) Å in $CuCl_2$·2L1 is consistent with the presence of a weak Cu–S bond such as those found in the 1,5,9-trithiacyclododecane[18] or 2,5,8-trithia[9](2,5)thiophenophane[19] complexes of copper(II).

Molecules of $CuCl_2$·L3 (Figure 3) have a distorted trigonal bipyramidal coordination sphere about copper. The equatorial plane is a plane of symmetry within which one of the chlorines is displaced ~30° from its expected position to give bond angles in the equatorial plane of 92.4(3) (O–Cu–Cl(2)), 135.7(3) (O–Cu–Cl(1)), and 131.9(2)° (Cl(1)–Cu–Cl(2)). The Cu–$Cl_{terminal}$ bond lengths of 2.240(4) and 2.253(4) Å are normal as are the Cu–S distances of 2.353(2) Å, but the Cu–O distance of 2.30(1) Å is approximately 0.3 Å longer than expected when compared to those of other trigonal bipyramidal copper(II) complexes[20-24]

Table IV. Positional and Thermal Parameters and Equivalent Isotropic Temperature Factors for $CuCl_2$·L3

atom	x	y	z	B_{eq}[a]
Cu	0.5184(1)	1/4	0.2040(2)	3.45(8)
Cl(1)	0.4430(3)	1/4	–0.0275(4)	4.0(2)
Cl(2)	0.6901(3)	1/4	0.2785(6)	6.1(2)
S(1)	0.5007(2)	0.1174(1)	0.2473(3)	3.9(1)
S(2)	0.4234(3)	–0.0649(2)	0.1407(4)	5.8(2)
O(1)	0.4581(9)	1/4	0.452(1)	4.8(6)
C(1)	0.411(1)	0.1828(6)	0.507(1)	5.4(6)
C(2)	0.479(1)	0.1173(6)	0.449(1)	5.0(6)
C(3)	0.3703(8)	0.0885(5)	0.178(1)	4.2(6)
C(4)	0.3448(7)	0.0061(5)	0.213(1)	3.3(5)
C(5)	0.2596(7)	–0.0220(5)	0.297(1)	4.0(5)
C(6)	0.267(1)	–0.1038(7)	0.298(1)	6.3(7)
C(7)	0.345(1)	–0.1328(5)	0.220(1)	5.3(6)

[a] B_{eq} (Å^2) is the mean of the principal axes of the thermal ellipsoid.

Table V. Selected Bond Lengths and Angles in $CuCl_2$·L3

Distances (Å)			
Cu–Cl(1)	2.240(4)	C(3)–S(1)	1.81(1)
Cu–Cl(2)	2.253(4)	C(2)–S(1)	1.79(1)
Cu–O	2.30(1)	C(1)–O	1.40(1)
Cu–S(1)	2.353(2)		
Angles (deg)			
Cl(1)–Cu–Cl(2)	131.9(2)	Cl(2)–Cu–S(1)	92.49(8)
Cl(1)–Cu–O	135.7(3)	O–Cu–S(1)	79.46(8)
Cl(1)–Cu–S(1)	96.08(8)	S(1)–Cu–S(1′)	158.5(2)
Cl(2)–Cu–O	92.4(3)		

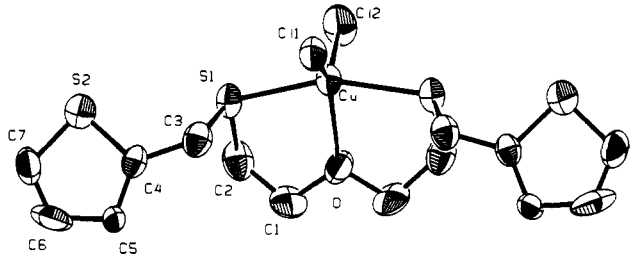

Figure 3. Molecular structure of $CuCl_2$·L3.

and the apex-to-apex angle (S(1)–Cu–S(1′) = 158.5(2)°) is ~22° less than ideal.

ESR spectra of microcrystalline samples of $CuCl_2$·2L1 and $CuCl_2$·L3 (Figure 4) are consistent with the two structures revealed by the X-ray studies. For $CuCl_2$·2L1, $g_\parallel = 2.15$ and $g_\perp = 2.04$ while, for $CuCl_2$·L3, $g_\perp = 2.16$ and $g_\parallel = 2.04$. The corresponding spectrum of $(CuCl_2$·$L2)_2$ is also shown in Figure 4 ($g_\parallel = 2.17$, $g_\perp = 2.05$). With these g values, no hyperfine coupling, and no signals near $g = 4$, it is similar to the spectrum of $CuCl_2$·2L1 and to spectra of dinuclear complexes we have described previously that have limited intramolecular coupling between their paramagnetic Cu(II) centers.[1,19] Those dinuclear species have strong IR absorptions at 300 and 250 cm^{-1} assigned to terminal (Cu–Cl) and bridging (Cu–Cl–Cu) vibrations. The same bands are found in spectra of $CuCl_2$·L2, but the 250-cm^{-1} band is absent or very weak in spectra of mononuclear $CuCl_2$·2L1 and $CuCl_2$·L3. An axial-to-equatorial linkage of coordination spheres in dinuclear five- or six-coordinated species disfavors antiferromagnetic coupling[1] and leads to ESR spectra and room-temperature magnetic moments typical of magnetically dilute Cu(II). For $CuCl_2$·L2, μ_{eff} at 24.8 °C is 1.88 μ_B and the complex shows no ESR signal near $g = 4$. In this respect, it resembles $CuCl_2$·2L1 (μ_{eff} = 1.87 μ_B at 22.6 °C) and $CuCl_2$·L3 (μ_{eff} = 1.86 μ_B at 23.1 °C), which also show no ESR signals near $g = 4$. On the basis of these observations, the structure proposed for the compound of empirical formula $CuCl_2$·L2 is as shown in Figure 5a.

(16) Cohen, B.; Ou, C. C.; Lalancette, R. A.; Borowski, W.; Potenza, J. A.; Schugar, H. J. *Inorg. Chem.* **1979**, *18*, 217.
(17) Baker, E. N.; Norris, G. E. *J. Chem. Soc., Dalton Trans.* **1977**, 877.
(18) Rawle, S. C.; Admans, G. A.; Cooper, S. R. *J. Chem. Soc., Dalton Trans.* **1988**, 93.
(19) Lucas, C. R.; Liu, S.; Newlands, M. J.; Charland, J. P.; Gabe, E. J. *Can. J. Chem.* **1989**, *67*, 639.
(20) Drew, M. G. B.; Yates, P. C.; Esho, F. S.; Trocha-Grimshaw, J.; Lavery, A.; McKillop, K. P.; Nelson, S. M.; Nelson, J. *J. Chem. Soc., Dalton Trans.* **1988**, 2995.
(21) Chiari, B.; Piovesana, O.; Tarantelli, T.; Zanazzi, P. F. *Inorg. Chem.* **1988**, *27*, 3246.
(22) Woon, T. C.; McDonald, R.; Mandal, S. K.; Thompson, L. K.; Connors, S. P.; Addison, A. W. *J. Chem. Soc., Dalton Trans.* **1986**, 2381.
(23) Hathaway, B. J.; Billing, D. E. *Coord. Chem. Rev.* **1970**, *5*, 143.
(24) Hathaway, B. J. *Coord. Chem. Rev.* **1981**, *35*, 211.

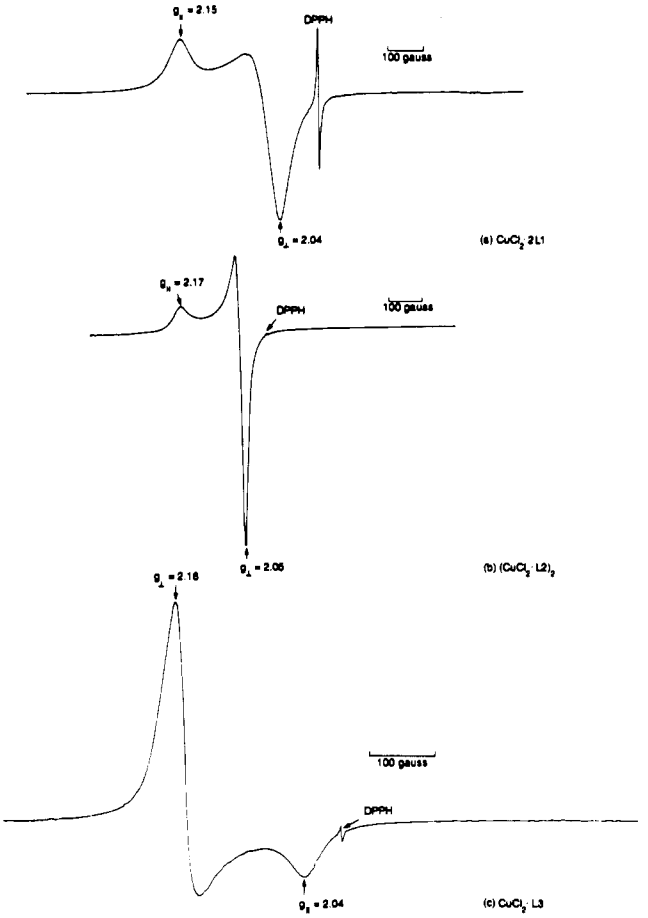

Figure 4. X-band ESR spectra of microcrystalline $CuCl_2$·2L1 (a), $(CuCl_2$·L2$)_2$ (b), and $CuCl_2$·L3 (c).

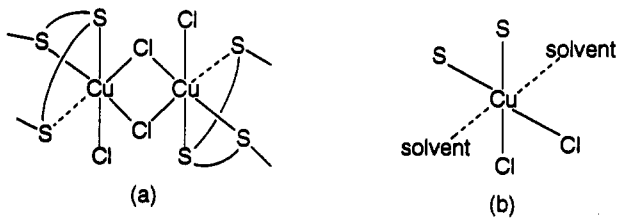

Figure 5. (a) Proposed structure of solid $(CuCl_2$·L2$)_2$ and (b) proposed coordination sphere of solvated complexes in CH_2Cl_2.

Table VI. Electronic Spectroscopic Data

	λ_{max}, nm (ϵ)			
		solution		
complex	solid[a]	CH_2Cl_2	CH_3CN	assgnt
$CuCl_2$·2L1		950 (sh)		d–d
	590	740 (70)	730 (80)	d–d
	440	440 (360)	440 (600)	S → Cu
	325	330 (900)	310 (2000)	Cl → Cu
$(CuCl_2$·L2$)_2$		950 (sh)		d–d
	600	755 (85)	725 (70)	d–d
	435	435 (360)	420 (700)	S → Cu
	300	325 (1040)	300 (2000)	Cl → Cu
$CuCl_2$·L3		925 (sh)		d–d
	790	720 (75)	725 (65)	d–d
	425	435 (500)	430 (500)	S → Cu
	320	330 (sh)	300 (1500)	Cl → Cu

[a] Nujol mulls.

Data and assignments for the solid-state (Nujol mull) electronic spectra of the three complexes are given in Table VI. The d–d band envelope is red-shifted ~200 nm in $CuCl_2$·L3 due to its trigonal bipyramidal geometry compared to the case of the other two tetragonally distorted octahedral species. In other respects, the spectra are similar, and therefore, the weakly bound axial

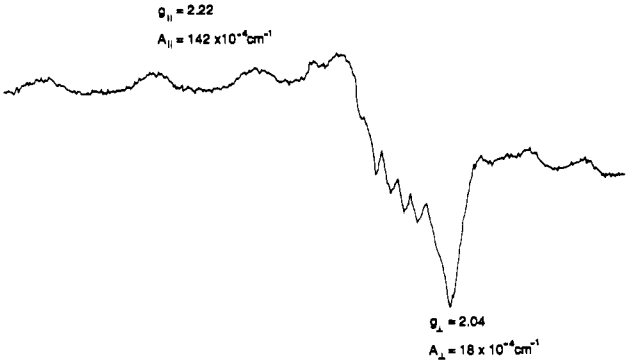

Figure 6. X-band ESR spectrum at 77 K of $CuCl_2$·L3 in CH_2Cl_2 glass.

S-donors in $CuCl_2$·2L1 and (presumably) $(CuCl_2$·L2$)_2$ have little effect on the solid-state spectra. The "effective" chromophore in the solid state is, therefore, $CuCl_2S_2$.

In solution, the compounds appear even more similar although some solvent-dependent characteristics may be noted (Table VI). For example, d–d bands of $CuCl_2$·L3 in solution are more like those of the other two compounds than was the case for the solids, suggesting loss of its trigonal bipyramidal structure upon dissolving. This structure change is confirmed by the ESR solution spectrum (Figure 6) assuming that the frozen solution "glasses" are representative of the solution state. The electronic and ESR spectra of $CuCl_2$·L3 in CH_2Cl_2 are therefore consistent with a solvated structure for the coordination sphere of $CuCl_2$·L3 like that shown in Figure 5b. Similarity of the solution electronic spectra for $(CuCl_2$·L2$)_2$ and $CuCl_2$·2L1 to each other and to that of $CuCl_2$·L3, while differing significantly from their solid-state spectra, suggests related solvated structures for all three coordination spheres (Figure 5b). Thus, for $(CuCl_2$·L2$)_2$, dissolving in CH_2Cl_2 involves cleavage of chlorine bridges between the copper centers with solvation in the opened coordination site while for $CuCl_2$·2L1, at least one of the long Cu–S bonds apparently dissociates to be replaced by a solvent interaction. When the solvent is replaced by CH_3CN, changes in the d–d bands occur, the cause of which is revealed by cyclic voltammetry.

For all three compounds, cyclic voltammograms recorded in CH_2Cl_2 are similar and characteristic of EC processes. A typical example for $CuCl_2$·L3 is shown in Figure 7. Values of ΔE_p = 182 mV and i_{pa}/i_{pc} = 0.34 at a sweep rate of 50 mV/s show the irreversible nature of the one-electron reduction process, but as sweep rate is increased, i_{pa}/i_{pc} increases. Processes consistent with the cyclic voltammetry and with the UV/vis and ESR data described earlier are shown in eqs 1 and 2.

$$CuCl_2\cdot L + e^- \rightleftarrows [CuCl_2\cdot L]^- \quad (1)$$

$$[CuCl_2\cdot L]^- \rightarrow CuCl\cdot L + Cl^- \quad (2)$$

In contrast, CH_3CN solutions give cyclic voltammograms in all three cases that are characteristic of quasi-reversible processes. An example for $CuCl_2$·L3 is shown in Figure 7. A process consistent with the cyclic voltammetry and with the higher energy d–d and Cl → Cu charge-transfer bands of spectra collected in CH_3CN (Table VI) is shown in eq 3.

$$[CuCl\cdot L]^+ + e^- \rightleftarrows [CuCl\cdot L] \quad (3)$$

Thus, in CH_2Cl_2 both Cu–Cl bonds are intact whereas in the more nucleophilic solvent, CH_3CN, one chlorine appears to have been displaced by solvent. In order to confirm this interpretation of the cyclic voltammetric data, conductance studies were

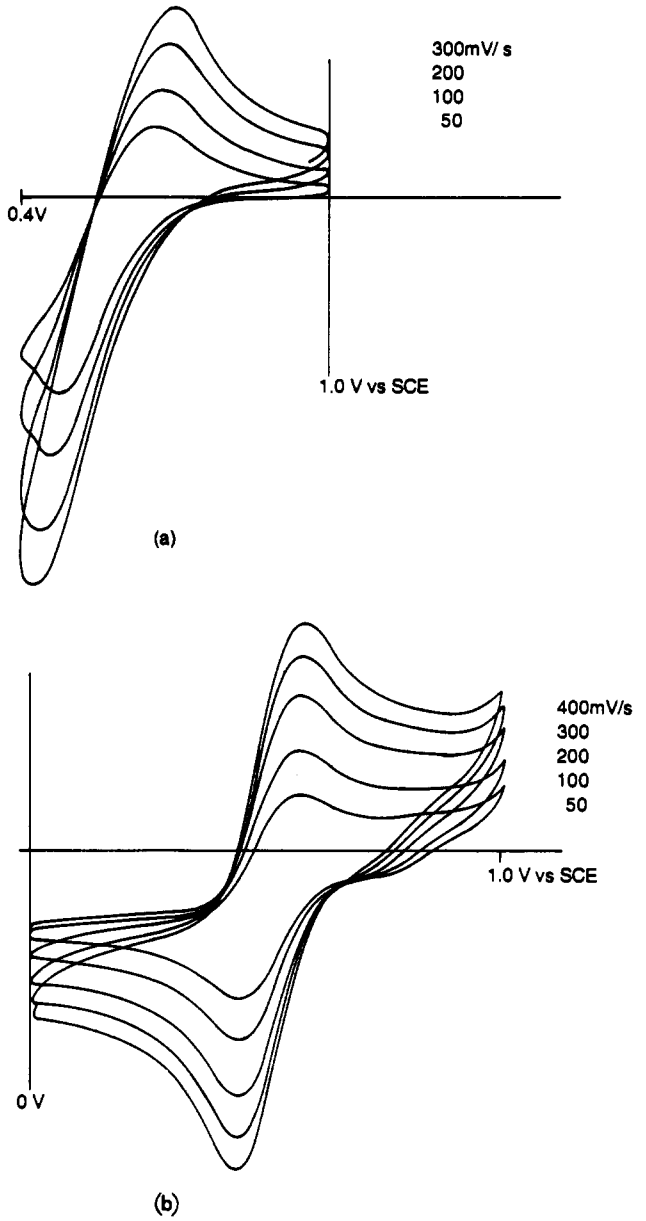

Figure 7. Cyclic voltammograms of $CuCl_2$·L3 in (a) CH_2Cl_2 and (b) CH_3CN.

undertaken in CH_3CN solution. The results are displayed as Onsager plots[25] in Figure 8. Slopes of these plots show clearly that $(CuCl_2·L2)_2$ and $CuCl_3$·L3 behave as 1:1 electrolytes in CH_3CN, as predicted. The data for $CuCl_2$·2L1, however, produce a curve rather than a straight line when Λ is plotted versus $\sqrt{C}$. This could indicate reversible dissociation of a second chloride or an entire ligand molecule. It is possible the different behavior of $CuCl_2$·2L1 is due to the fact that coordination of L1 is via one weak and one strong Cu–S bond per ligand rather than two or more strong bonds as is the case for L2 and L3, so that solvolysis proceeds via intermediates involving chelated ligands L2 and L3 but unidentate L1.

In *N,N*-dimethylformamide, reversible dissociation involving Cu–S bonds is revealed by ESR spectroscopy at 77 K (Figure 9). The ESR spectra show two species (1 and 2), relative concentrations of which are dependent upon total solute concentration. Species 1 has spectral characteristics identical to those we have detected under similar experimental conditions for *N,N*-dimethylformamide solutions containing $CuCl_2$ and any of eight macrocyclic or open-chain ligands having two or more thioether

(25) Feltham, R. D.; Hayter, R. G. *J. Chem. Soc.* **1964**, 4587.

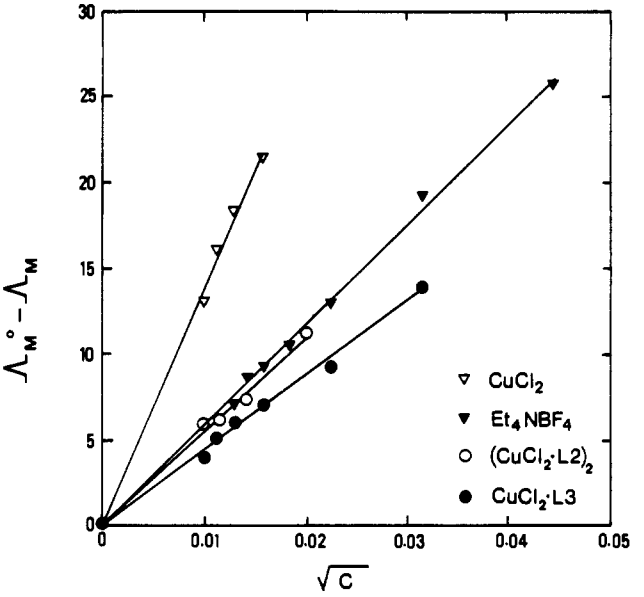

Figure 8. Onsager plots for solutions in CH_3CN.

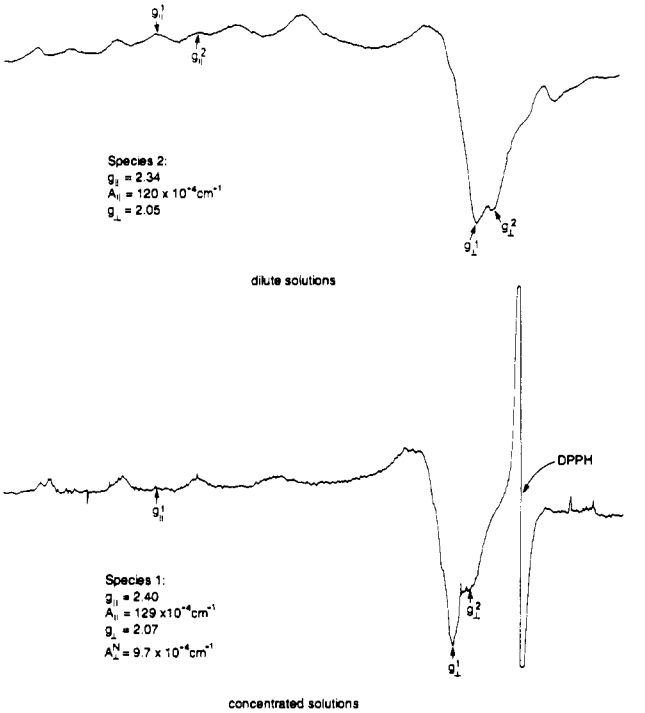

Figure 9. X-band ESR spectra at 77 K of $CuCl_2$·2L1 in *N,N*-dimethylformamide glass.

donor sites. Species 2 has a spectrum identical to that of anhydrous $CuCl_2$ in our hands, and it is known that under these conditions $CuCl_2$ dissociates one Cl^- and exists as a solvate.[26] Superhyperfine structure in the form of five lines on $g_{\perp}$ suggests interaction with two nitrogen atoms in a plane perpendicular to the principal axis and arises presumably from solvation of the copper species. An equilibrium such as that shown in eq 4 is consistent with these ESR results and is similar to one we have observed previously in systems involving N_2S_3 or N_2S_2O donors.[5]

$$n\text{DMF} + [\text{CuCl·L}]^+ \rightleftarrows [\text{CuCl·}n\text{DMF}]^+ + \text{L} \qquad (4)$$

Conclusions

Complexes of $CuCl_2$ with O- and S-donors undergo significant structural changes upon being dissolved. The nature and extent

(26) Kadish, K. M.; Deng, Y.; Zaydoun, S.; Idrissi, M. S. *J. Chem. Soc., Dalton Trans.* **1990**, 2809.

of these changes depend upon the characteristics of the solvent and the concentration of the solution. In poorly coordinating solvents such as CH_2Cl_2, ligand donor atoms may be displaced but only if they are weakly bound. Dimers may be cleaved to monomers and five-coordinate species may become six-coordinate solvates. In more nucleophilic solvents such as CH_3CN or *N*,*N*-dimethylformamide, dissociation of a Cu–Cl bond may occur as may reversible dissociation of Cu–S and Cu–O bonds, leading ultimately in dilute solutions to predominantly $[CuCl\cdot n(solvent)]^+$ and free ligand. Changes in electronic spectra as a result of dissolving may be significant or subtle depending upon the type of solvent used and the solid-state structure of the complex. These changes are therefore not always reliable indicators of structural change induced by dissolving. ESR spectroscopy, however, is a more sensitive probe and, when taken with other physical data, can provide good indication of even small changes in the coordination sphere of a metal that occur as a result of dissolving. The results suggest that modeling hydrophobic active sites of copper-containing enzymes by using simple models dissolved in nonaqueous solvents may be difficult because the coordination spheres detected in the solid state are usually not the same in solution. Successful modeling may require ligands with multidentate donor sites in "pockets" into which the metal ion may be placed with reasonable assurance that its coordination sphere geometry will only change as a result of oxidation and not merely as a consequence of solvation or ion pairing in solution.

Acknowledgment. Financial support by the Natural Sciences and Engineering Research Council of Canada and by Memorial University of Newfoundland is gratefully acknowledged.

Supplementary Material Available: A textual presentation of the X-ray studies and tables giving crystal data and details of the structure determination, bond lengths, bond angles, anisotropic thermal parameters, and hydrogen atom locations (20 pages). Ordering information is given on any current masthead page.